Sliding-Mode Control of a Nonlinear-Input System: Application to a Magnetically Levitated Fast-Tool Servo

Hector M. Gutierrez, *Member, IEEE*, and Paul I. Ro

***Abstract*—Magnetic servo levitation (MSL) is currently being investigated as an alternative to drive fast-tool servo systems that could overcome the range limitations inherent to piezoelectric driven devices while operating over a wide bandwidth. To control such systems, a feedback-linearized controller coupled with a Kalman filter has been previously described. Performance limitations that degrade tracking accuracy suggest the use of a more robust controller design approach, such as sliding-mode control. Current literature on sliding mode deals almost exclusively with systems that are affine on the input, while the magnetic fast-tool servo is nonlinear on it when the control action is current command. This paper discusses a sliding-mode-based controller that overcomes the aforementioned problem by defining a modified sliding condition to calculate control action. Experimental results demonstrate the feasibility of achieving long-range fast tracking with magnetically levitated devices by using sliding-mode control.**

***Index Terms*—Fast-tool servo systems, magnetic servo levitation, nonaffine systems, sliding-mode control.**

I. Introduction

MAGNETIC SERVO levitation (MSL) [4], [7], [8], [20]–[22] represents a promising but very challenging alternative to actuate positioning systems where both long range and fast response (wide bandwidth) are required. Several applications require high-speed, high-resolution, high-stiffness positioning actuators. For these applications, piezoelectric actuators have been used extensively, providing excellent performance, but they are severely restricted in range of travel. Piezoelectric stacks are also difficult to mount and pose problems related to mechanical design, cost, and cooling. For longer ranges of motion, linear motors have been used, but the maximum force and bandwidth available are very limited. MSL is a form of electromagnetic actuation that uses the attractive forces rather than the Lorentz (shear) forces utilized by most electromagnetic motors (see Fig. 1). Much higher forces are possible, but the range of motion is smaller and the system is inherently unstable and highly nonlinear. It is important to emphasize the need of both an accurate model and a robust control law if high positioning accuracy is expected. An active tool holder (fast-tool servo) based on MSL is depicted in Fig. 2. This type of actuator can be used in machining operations such as diamond turning of nonrotationally symmetric surfaces.

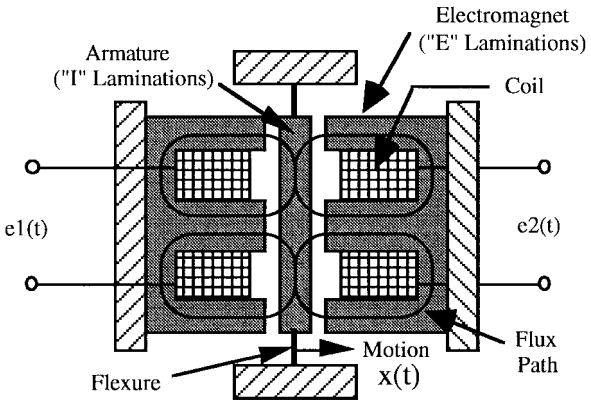

Fig. 1. Electromagnetic actuator based on attractive force.

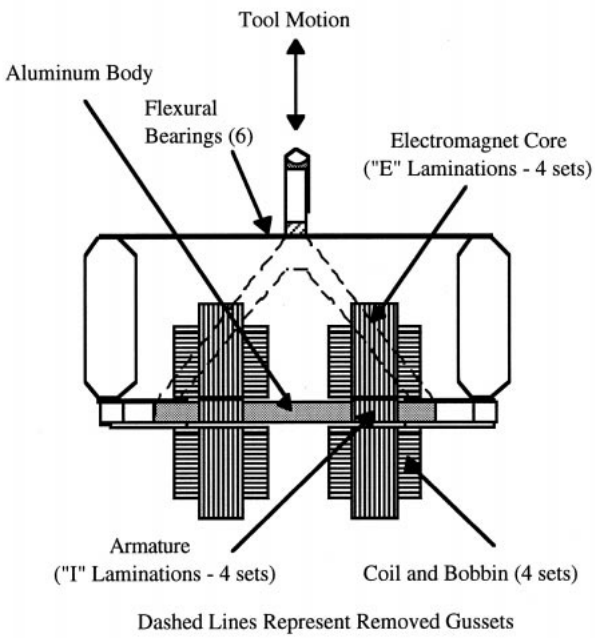

Fig. 2. Actuator schematic.

Most of the currently existing magnetically levitated devices are used for regulation tasks and not for tracking (maglev vehicles, magnetic suspension systems). Long-range wide-band tracking clearly represents a more difficult problem.

Manuscript received June 2, 1997; revised May 1, 1998. Abstract published on the Internet August 25, 1998.

H. M. Gutierrez is with the Center for Advanced Computing and Communications, North Carolina State University, Raleigh, NC 27695 USA.

P. I. Ro is with the Mechanical and Aerospace Engineering Department, North Carolina State University, Raleigh, NC 27695 USA.

Publisher Item Identifier S 0278-0046(98)08470-6.

II. Mathematical Model of the Electromagnetic Actuator

A novel mathematical model of the nonlinear current–force interaction for long-range displacements has been proposed [4] and used to synthesize a nonlinear controller based on feedback linearization [4], [18]. Some of the problems highlighted by such approach is the controller sensitivity to parameter variations and unmodeled dynamics. Such performance limitations suggest the use of a more robust controller design technique, such as variable-structure sliding-mode control.

Electromechanical systems driven by magnetic forces, such as magnetic bearings or micropositioning stages [19], typically have a very small range of motion (in the order of a few micrometers) and small bandwidth (in the order of a few hertz). For this reason, simple mathematical models of the magnetic force seem to work reasonably well, for instance,

$$F_{\text{mag}} = K\frac{i^2}{g^2}$$

where i is coil current, g is air gap, and K is some constant to be determined. Furthermore, some of these systems operate at high bias current levels, allowing the use of Jacobian (small signal) linearization. A long-range actuator, where displacement can not be described as small perturbations of a nominal trajectory, requires a model that is accurate over a wide range of displacement and frequencies.

An electromagnetic actuator is a coupled system where motion equations must be solved simultaneously with electromagnetic and circuit equations. Strong coupling models are given by incorporating the motion equations into a finite-element model (FEM) of the electromagnetic equations. In parametrization coupling models, the electromagnetic field equations are solved off-line by finite-element methods to determine magnetic force and flux as static functions of current and position [15]. The solutions are then used to solve the circuit and motion equations by interpolating parameter values (force, flux) according to measured position and current. Although FEM-based models have the appeal of being based on first principles of physics, they all involve a number of approximations and are sensitive to both structural and material parameter uncertainties. They do not consider more complex effects, such as material anisotropy, mechanical misalignment, eddy-current losses, hysteresis, or thermal effects. For long-range, wide-bandwidth, high-precision applications, these methods are not accurate enough. This prompts the development of a different modeling strategy.

A model of the magnetically levitated servo system can be formulated in such a way that nonlinearities are separable and additive

$$a_1\frac{d^2x}{dt^2} + a_2\frac{dx}{dt} + a_3x = F_{\text{mag2}} - F_{\text{mag1}} \tag{1}$$

where x is displacement, a_i are unknown parameters, and each magnetic force F_{mag} can be described as some polynomial of coil current (i) and the corresponding air gap. For instance,

$$F_{\text{mag2}} = \sum_{j=1}^{n}\left(K_{1j}\frac{i_2}{(x_o - x)^{0.5j}} + K_{2j}\frac{i_2^2}{(x_0 - x)^{0.5j}}\right) \tag{2}$$

where x is measured from the equilibrium position, x_o is the nominal air gap, and K_{ij} are parameters to be determined. The problem consists on finding the unknown coefficients in (1) and (2) such that experimental input–output sequences can be fitted in a minimum mean-square-error sense. To use linear parametric techniques to find optimal fits for these parameters, each rational term in (2) can be considered a separate input to the system, such that (1) can be written as

$$\frac{d}{dt}\begin{bmatrix} x \\ \dfrac{dx}{dt}\end{bmatrix} = \begin{bmatrix} 0 & 1 \\ -\dfrac{a_3}{a_1} & -\dfrac{a_2}{a_1}\end{bmatrix}\begin{bmatrix} x \\ \dfrac{dx}{dt}\end{bmatrix} + \begin{bmatrix} 0 & 0 & \cdots & 0 \\ K_{11} & K_{21} & \cdots & K_{4n}\end{bmatrix}\begin{bmatrix} u_1 \\ u_2 \\ \cdots \\ u_{4n}\end{bmatrix}. \tag{3}$$

The techniques used to estimate the parameters involved are called prediction error methods [14] and are based on the minimization of a cost function which is the sum of the squared prediction errors. Previous knowledge or "reasonable guesses" of the system's parameters (e.g., effective mass, estimated spring stiffness) significantly improve the speed of convergence and minimize the chance of hitting local minima since they provide "good" initial estimates to the algorithm. This procedure converges to a unique set of parameters and, therefore, models the system as time invariant. Model parameters of the MSL servo were determined by exciting the system with band-limited noise and recording the corresponding I/O sequences. Parameters of the system model (3) were then estimated using the Gauss–Newton algorithm. More details and experimental results can be found in [4] and [5].

III. Controller Design for Magnetic Levitation Via Feedback Linearization

The model structure (2), (3) is particularly well suited for feedback linearization, as described in [18]. This is an approach to nonlinear controller design that differs entirely from conventional linearization (i.e., small-signal analysis) in the sense that linearization is achieved by exact state transformations and feedback, rather than by a linear approximation of the dynamics. The system is not constrained to operate around some nominal trajectory, nor must the input signal be "small" compared to the input bias level. Applications that use Jacobian linearization (such as most magnetic bearing controllers) require biasing currents approximately ten times larger than the control current in order to achieve reasonable performance.

The MSL fast-tool servo can be feedback linearized by the following input coordinate transformation:

$$\begin{aligned}\frac{dX}{dt} &= AX + f(X, i_1, i_2) \\ &= AX + f(X, U) \Leftrightarrow \\ \frac{dX}{dt} &= AX + \begin{bmatrix} 0 & 0 \\ 1 & 1\end{bmatrix}\begin{bmatrix} v_1 \\ v_2\end{bmatrix}\end{aligned} \tag{4}$$

where $f(X, U)$ represents the input nonlinearity described by (2). The problem becomes a standard linear controller design problem, and the performance is limited by the range

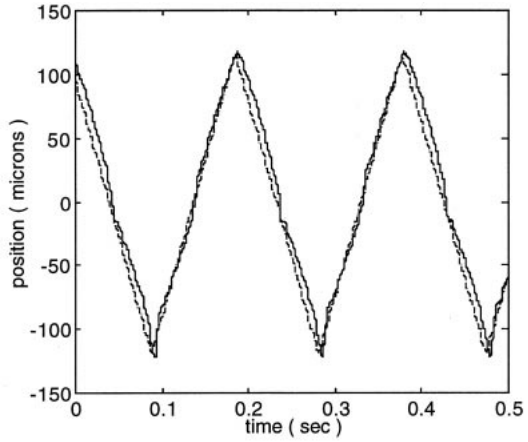

Fig. 3. Feedback linearization. Response to ramp command, 5 Hz (reference command: dashed line, measured response: solid line).

of the input space $\langle v_1, v_2 \rangle$ over which the inverse map $i = f^{-1}(X, v)$ is well defined. To further clarify this point, consider again (1) and (2). Terms containing input currents can be factored as follows:

$$a_1 \frac{d^2x}{dt^2} + a_2 \frac{dx}{dt} + a_3 x = K_1(x) i_1 + K_2(x) i_1^2 + K_3(x) i_2 + K_4(x) i_2^2. \quad (5)$$

The following input coordinate transformation becomes obviously convenient:

$$\begin{aligned} v_1 &= K_3(x) i_1 + K_4(x) i_1^2 \\ v_2 &= K_1(x) i_2 + K_2(x) i_2^2 \end{aligned} \quad (6)$$

which renders the system linear as in (4). Once the system is linearized, controller design can be carried out based on a linear quadratic regulator (LQR), using a reduced-order discrete Kalman filter to estimate velocity. To eliminate steady-state error, the integral of the tracking error was included as an additional state, to take advantage of the regulatory capabilities of the LQR algorithm.

Feedback linearization as described above has been implemented and tested on the magnetically levitated fast-tool servo. Tracking performance is illustrated in Figs. 3 (maximum range) and 4 (positioning resolution). In both plots, command signal is shown as a dashed line and measured response as a solid line.

One significant achievement of this approach is the ability to achieve good tracking over a wide range of travel (resolution can be up to 200 nm over a 240-μm range). Tracking performance, however, degrades when either range or frequency bounds are exceeded. Performance degradation is illustrated in Fig. 5, where measured output (position) appears distorted in addition to the frequency-dependent phase lag inherent in any linear controller.

To examine model error as a possible factor of performance degradation, input coil currents were recorded while operating the system in closed loop. Coil current data was later sent through a simulation network corresponding to the parametric model [(2), (3)] to evaluate the ability of the model to reproduce the behavior of the actual plant. Results are shown

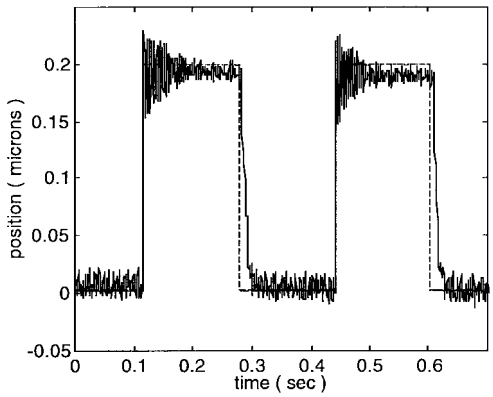

Fig. 4. Feedback linearization. Step response, 200 nm (reference command: dashed line, measured response: solid line).

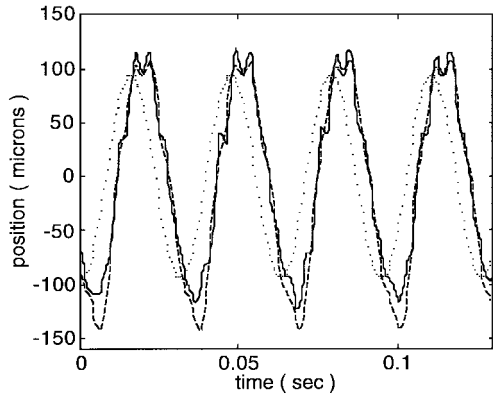

Fig. 5. Feedback linearization. Performance degradation (command: dotted line, measured output: dashed line, simulated output: solid line).

in Fig. 5. While simulated output tends to track actual output, the observed prediction error can be as large as 30 μm when tracking a 180-μm (PV) sine-wave command. Output distortion worsens whenever the system is operated under conditions that make model error grow.

Frequency response of the closed-loop system was measured using a spectrum analyzer and is shown in Fig. 6. Good tracking (not less than $-$0.5-dB gain with a phase lag of 20° or smaller) can be achieved only up to 10 Hz (the design goal was 300 Hz).

While these results illustrate both the feasibility of achieving long-range tracking with a magnetically levitated device and the adequacy of the parametric model, there are a number of factors that degrade overall performance. Feedback linearization is very sensitive to parameter uncertainties, unmodeled dynamics, and closed-loop rate. Computational delay and A/D–D/A conversion delays also have a significant impact on tracking performance when the desired bandwidth is large compared to the available sampling rate. Domain boundaries imposed by the inverse maps [(see (6)], sensor noise, and amplifier bandwidth (frequency band where the power amplifiers behave as ideal current sources) also affect overall closed-loop performance. As is, the response of a linearized controller is not satisfactory for the intended application. Even if the model were perfect, the best (theoretical) performance of this

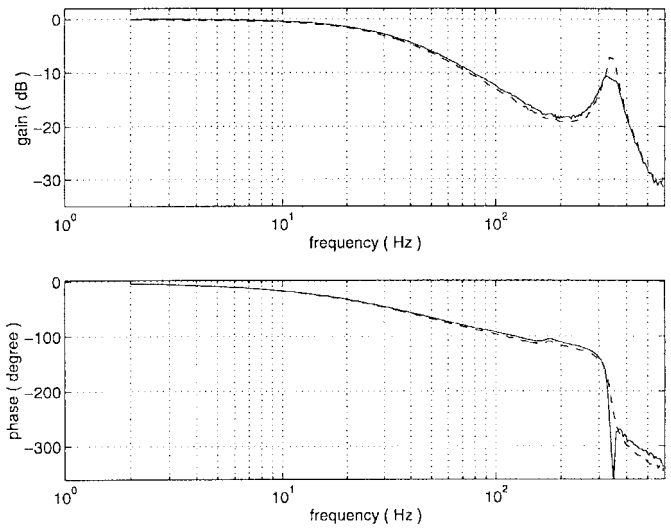

Fig. 6. Feedback linearization. Frequency response (measured response: solid line, least-squares linear fit: dashed line).

scheme is that of a linear controller, which hinders achieving the desired bandwidth with reasonable levels of control action.

IV. Controller Design for Magnetic Levitation Based on Sliding Mode

In recent years, variable-structure sliding-mode controller design [3], [10], [17], [18], [23] has drawn considerable attention from the control community. Sliding-mode design has several features that makes it an attractive alternative to solve tracking problems in nonlinear systems, the most important being its robustness to model uncertainties and unmodeled dynamics.

The mathematical foundations of sliding mode can be found in several recent publications [3], [17], [23]. Sliding-mode design can be interpreted in several ways. One way of looking at it is to think of the design process as a two-step procedure. First, a region of the state space where the system behaves as desired is defined (sliding surface design). Then, a control action that takes the system into such surface and keeps it there is to be determined. Robustness is usually achieved based on a switched control law. The design of the control action can be attempted based on different strategies, a straightforward one being based on defining a Lyapunov-like condition that makes the sliding surface an attractive region for the state vector trajectories. For this discussion, consider first the time-varying surface $S(t)$ in the state space R^n

$$S(\vec{x},t)=\left(\frac{d}{dt}+\lambda\right)^{n-1}\tilde{x}=0 \tag{7}$$

where $\tilde{x}=\vec{x}-\vec{r}=[x-r \quad \dot{x}-\dot{r} \quad \cdots \quad (x^{(n-1)}-r^{(n-1)})]^T$ is the tracking error vector, λ is some positive constant, and n is the relative degree of the system [18]. Any state trajectory x that lies on this surface tracks the reference r, since (7) defines a differential equation on the error vector that stably converges to zero.

There are several possible strategies to design the control action u that takes the system to the surface defined by (7). One such strategy is to define u in such a way that S becomes an attractive region for the state trajectories, for instance, by forcing the control action to satisfy a geometric condition on the distance to S as measured by S^2

$$\frac{1}{2}\frac{d}{dt}(s^2)\le-\eta|s| \Leftrightarrow s\frac{ds}{dt}\le-\eta|s|\le 0 \tag{8}$$

where η is a strictly positive constant. This condition forces the squared "distance" to the surface to decrease along all state trajectories [18] or, in other words, all the state trajectories are constrained to point toward S.

A. Sliding-Mode Design for the MSL System in Current Mode

So far, the model used for controller design [(1), (2)] considers current command as the available control action. This will be referred to as current mode operation. A power amplifier that resembles an ideal current source within the frequency band of interest will be required. Current literature on sliding mode deals almost exclusively with systems that are affine on the input and either are on companion form or can be converted to it by some nonlinear coordinate transformation. This is

$$\vec{x}^{(n)}=f(\vec{x})+B(\vec{x})u.$$

It is obvious from (2) that this is not the case for the MSL system. The approach suggested here is inspired by [2]. Consider a nonlinear system that is nonaffine in the input

$$\frac{d\vec{x}}{dt}=f(\vec{x})+Bh(i), \qquad \vec{x}\in R^n \tag{9}$$

where $h(i)$ is some nonlinear function of the control command i, and B is a coefficient matrix of adequate dimensions, e.g., if there were p states to be tracked, h would be $px1$ and B would be nxp. A corresponding first-order sliding surface is

$$S(\vec{y},t)=(\dot{\vec{y}}-\dot{\vec{r}})+\Lambda(\vec{y}-\vec{r}), \qquad \vec{y}=C\vec{x}, \quad y\in R^p \tag{10}$$

where $\Lambda=\text{diag}(\lambda_1,\cdots,\lambda_p)$, and $\vec{y}$ is formed by the components of the state vector that are to be tracked. The sliding condition (8), can be rewritten as

$$S^T\frac{dS}{dt}=S^T\left(\frac{\partial S}{\partial\vec{x}}f+\frac{\partial S}{\partial\vec{x}}Bh(i)+\frac{\partial S}{\partial t}\right)<0. \tag{11}$$

Define

$$D_{pxp}=\frac{\partial S}{\partial\vec{x}}B; \qquad S^*=D^TS\Leftrightarrow S^T=(S^*)^TD^{-1} \tag{12}$$

and, also,

$$\rho(\vec{x})=D^{-1}\left(\frac{\partial S}{\partial\vec{x}}f+\frac{\partial S}{\partial t}\right). \tag{13}$$

By replacing (12) and (13) in (11), a modified sliding condition, equivalent to (8), is defined

$$(S^*)^T(h(i)+\rho(\vec{x}))<0. \tag{14}$$

To use (14) to define a control action for the MSL system that will take the state trajectories to S, it will be assumed that

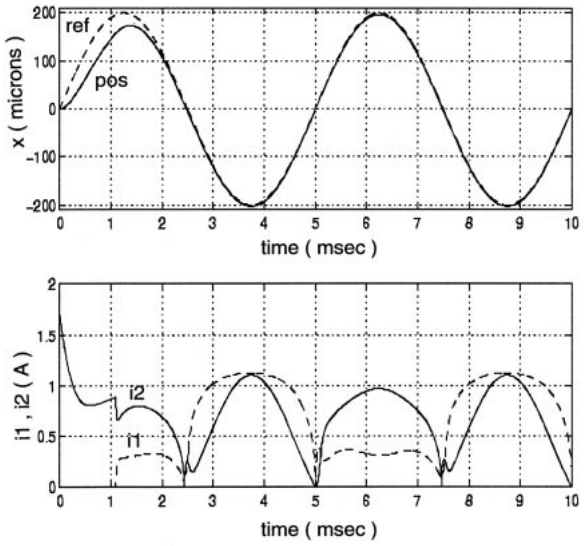

Fig. 7. Tracking performance, (16) 200-μm sine wave at 200 Hz.

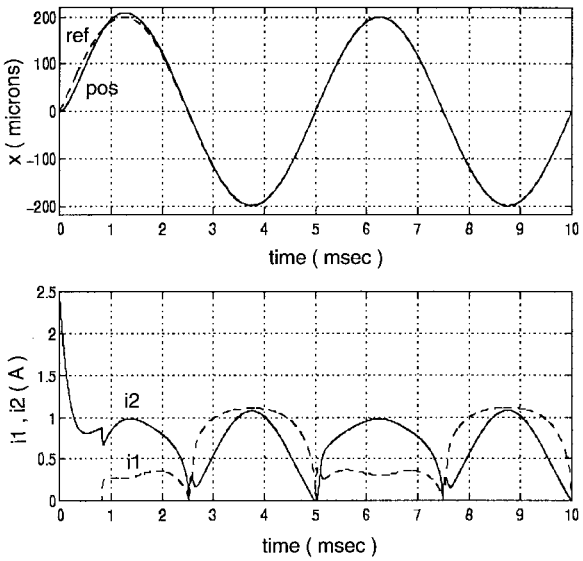

Fig. 8. Tracking performance, 200-μm sine wave at 200 Hz. Sliding surface includes integral error term.

it is possible to represent the magnetic forces as

$$F_1 = h_1(i_1) = b_1 \frac{i_1^2}{(x_1 + x)^2}, \quad F_2 = h_2(i_2) = b_2 \frac{i_2^2}{(x_2 - x)^2} \tag{15}$$

where F_1 is the force exerted by the left-side magnets, F_2 is the corresponding right-side force, x_1 and x_2 are the equilibrium gaps at each side, x is the actuator position, and $b_1 < 0$, $b_2 > 0$ are time-varying coefficients with known bounds.

In current mode, the MSL system can be treated as a single-input–single-output (SISO) system, with only one pair of magnets active at any given time, depending on the sign of the tracking error. In this case, $D = 1$ and, hence, $S = S^*$. From this, the following control algorithm is proposed:

$$i_1 = \sqrt{\frac{-n(\vec{x})(x_1 + x)^2}{\max b_1}}, \qquad i_2 = 0; \text{ if } S > 0$$
$$i_2 = \sqrt{\frac{n(\vec{x})(x_2 - x)^2}{\min b_2}}, \qquad i_1 = 0; \text{ if } S < 0 \tag{16}$$

where $n(\vec{x})$ is some scalar function of the sate vector such that

$$0 < |\rho(\vec{x})| < n(\vec{x}). \tag{17}$$

To see how (16) meets the modified sliding condition (14), two cases need to be analyzed. For $S > 0$, the current i_1 must be squared, and the resulting equation solved for $n(\vec{x})$. The corresponding expression represents an upper bound for the magnetic force $h_1(i_1)$. Since $n(\vec{x})$ is an upper bound for $|\rho(\vec{x})|$, it can be established that $-h_1(i_1) > \rho(\vec{x})$; the sliding condition is, thus, satisfied. For $S < 0$, the procedure is similar.

The control algorithm (16) has been simulated to evaluate its performance. Bounds for b_1 and b_2 were obtained off-line from recorded I/O data corresponding to exciting the open-loop system with band-limited noise. Tracking performance and the corresponding command currents are shown in Fig. 7. Notice that the sliding surface used corresponds to (10). Plant equations used for these simulations correspond to the full-scale model corresponding to (1) and (2). Full state feedback is assumed (both position and velocity assumed available).

To further penalize tracking error, an integral term can be added to the sliding surface. For instance, (7) can be rewritten for the case $n = 3$

$$s(\vec{x}, t) = \left(\frac{d}{dt} + \lambda\right)^2 \left(\int_0^t (x - r)\, dt\right)$$
$$= (\dot{x} - \dot{r}) + 2\lambda(x - r) + \lambda^2 \int_0^t (x - r)\, dt = 0. \tag{18}$$

Defining the sliding surface as in (18) redefines $\partial S/\partial \vec{x}$, $\partial S/\partial t$, and $\rho(\vec{x})$ accordingly. The control command can be shown to still be given as in (16). The resulting algorithm was also simulated to evaluate its performance; tracking response and the corresponding command currents are shown in Fig. 8. Once again, the plant corresponds to the full-scale model, and full state feedback is assumed.

Both controllers used in this section incorporate a constant thickness boundary layer (as described in [17], [18], and [23]) to reduce control chattering. The boundary layer is a modification of the control algorithm that allows switching around the sliding surface using a continuous function, avoiding the high control chatter that would result from attempting infinitely fast switching as the direct implementation of (16) could require. Within a boundary layer of thickness ϕ, the output of the controller is given by (16), scaled proportionally to the ratio (s/ϕ). If the entire trajectory lies within the boundary layer, both magnets are active at all times, as seen in Figs. 7 and 8. This obviously represents a tradeoff between the demand placed on the power amplifiers due to fast switching and the electric power dissipated on the device.

Figs. 7 and 8 illustrate the theoretical tracking capabilities of this controller and the corresponding current commands necessary to achieve such performance in the absence of noise or unmodeled dynamics. Although perfect tracking can theoretically be achieved by this design, several implementation

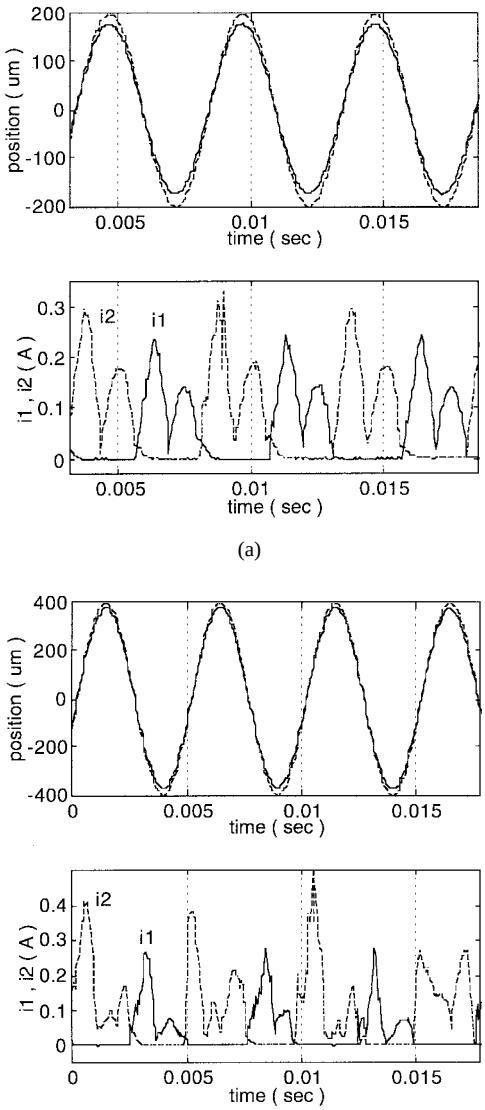

Fig. 9. (a) Tracking performance: 400-μm travel at 200 Hz and (b) tracking performance: 800-μm travel at 200 Hz.

issues degrade the potential performance. Speed estimation is a critical factor; an observer or some other estimation algorithm has to be included in the design. Control action chattering worsens due to noise, model uncertainties, parameter variations, performance of the state estimator, computational and conversion delays, etc. A tradeoff between control chattering, tracking accuracy, and power dissipation must eventually be established.

V. Experimental Results

The current-mode sliding controller has been implemented to control the magnetically levitated fast-tool servo depicted in Fig. 2, using an integral error term, as described by (18). Tracking performance and the corresponding current commands are shown in Fig. 9(a) and (b). In all displacement plots, command reference is shown as a dotted line and measured output as a solid line.

To achieve long-range tracking without overloading the power amplifiers due to fast switching, it is necessary to include a constant thickness boundary layer. Results shown in Fig. 9 correspond to $\lambda = 720$ and ϕ (boundary layer thickness) equal to 0.05. Linearity of the closed-loop response over the longer range of motion is shown in Fig. 10.

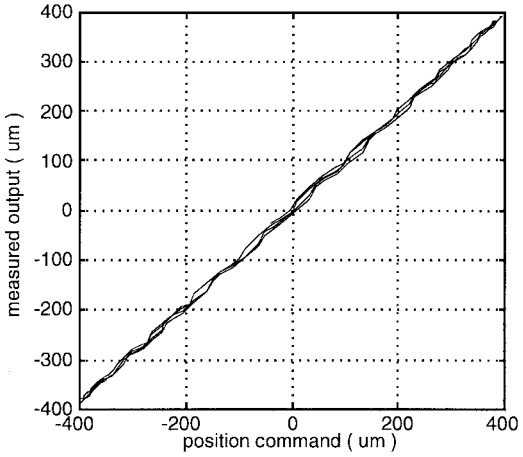

Fig. 10. Linearity of the closed-loop response, 800-μm travel at 200 Hz.

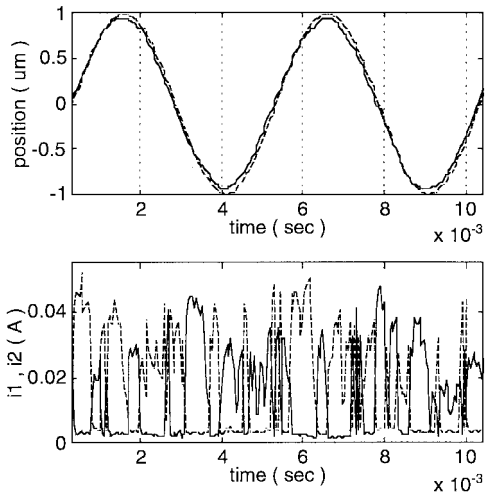

Fig. 11. Tracking performance: 2-μm travel at 200 Hz.

This control algorithm can also provide high-resolution positioning accuracy. In the submicrometer range, the boundary layer has to be very thin to allow for high-resolution tracking; since the control commands are also very small, the resulting fast switching is better tolerated by the amplifiers. A sample of results is shown in Fig. 11, where $\lambda = 760$ and $\phi = 10^{-9}$.

Some of the more relevant features of this control algorithm are its capacity to achieve fast tracking over a wide range of motion and the fact that it has near-zero phase lag, as opposed to any linear controller. This is very desirable, since it provides performance that does not degrade at higher speeds and allows easier and better synchronization between the fast-tool servo and the spindle rotation. This controller provides significantly better tracking performance than previously reported linearization schemes, in spite of being based on a very simple force model (15). This further illustrates the robustness of sliding-mode design to unmodeled dynamics.

A limitation that needs to be mentioned is that, to achieve good performance with current commands that are feasible

to the power amplifier, the device has to be operated close to its resonant frequency. This limitation is not very critical for fast-tool servo applications, since the spindle is almost always operated at a constant speed, and it is relatively easy to adjust the resonant frequency of the fast-tool servo according to the required spindle speed. On the other hand, operating at resonance is very efficient in terms of power consumption and eliminates the need of cooling the fast-tool servo and other thermal drift problems. Heat dissipation in a fast-tool servomechanism is a pressing issue and motivated the use of a purely switching control law (16) to avoid the additional rms current that would result from adding an equivalent control term (continuous control action that meets $dS/dt = 0$ and drives the system once sliding has been achieved). The use of a purely switching control law restricts the system to operate in a quasi-sliding mode [10].

VI. Conclusions

MSL represents a promising alternative to actuate long-range positioning systems while operating over a wide bandwidth. Feedback linearization with an augmented LQR compensator has been previously proposed, providing good tracking capabilities within a limited range and only at low frequencies. Robust controller design techniques are essential to minimize the effect of time-varying parameters and/or unmodeled dynamics and are being currently investigated. A sliding-mode algorithm has been presented that can achieve near perfect tracking over the desired range and frequency band. Several implementation issues, such as control action chatter, speed estimation, and computational time delay limit the ideal performance. It has been demonstrated that by operating at frequencies close to the resonance, high-speed long-range tracking is feasible. Since this is not a problem for fast-tool servo operation, the proposed controller allows the use of a novel actuation principle for long-range fast-tool servo applications, with the additional advantage of low power consumption.

References

[1] D. Cho, Y. Kato, and D. Spilman, "Sliding mode and classical control of magnetic levitation systems," *IEEE Contr. Syst. Mag.*, vol. 13, pp. 42–48, Feb. 1993.

[2] G. Conte and G. Orlando, "A variable structure control of a remotely operated vehicle," in *Proc. IEEE Conf. Ocean Engineering*, vol. 3, pp. 111–115.

[3] R. A. De Carlo, S. H. Zak, and S. V. Drakunov, "Variable structure, sliding mode controller design," in *IEEE Control Engineering Handbook.* Boca Raton, FL: CRC Press, 1995, pp. 941–951.

[4] H. M. Gutierrez and P. I. Ro, "Parametric modeling and control of a long-range actuator via magnetic servo levitation," *IEEE Trans. Magn.*, vol. 34, pp. 3689–3695, Sept. 1998.

[5] H. M. Gutierrez, B. A. Stancil, and P. I. Ro, "Design and modeling of a magnetically levitated fast-tool servo system for precision turning," in *Proc. ASME-IMECE,* 1995, pp. 491–497.

[6] J. K. Hedrick and W. H. Yao, "Adaptive sliding control of a magnetic suspension system," in *Variable Structure Control for Robotics and Aerospace Applications*, K. K. Young, Ed. Amsterdam, The Netherlands: Elsevier, 1993.

[7] T. Higuchi and M. Tsuda, "Design and control of magnetic servo levitation," *Rep. Inst. Ind. Sci. Univ. Tokyo*, vol. 37, no. 2, pp. 137–205, 1992.

[8] T. Higuchi, M. Tsuda, and Y. Nakamura, "Design of magnetic servo levitation for robot mechanisms," in *Proc. 20th Int. Symp. Industrial Robots,* 1989, pp. 136–144.

[9] T. Higuchi, H. Takahashi, K. Takahara, and S. Shingu, "Development of a magnetically suspended, tetrahedron-shaped antenna pointing system," in *Proc. 2nd Int. Symp. Magnetic Bearings,*, 1990, pp. 9–14.

[10] J. Y. Hung, W. Gao, and J. C. Hung, "Variable structure control of nonlinear systems," *IEEE Trans. Ind. Electron.*, vol. 40, pp. 45–55, Feb. 1993.

[11] L. S. Hung and S. C. Lin, "A multivariable sliding mode control for magnetic suspension systems," *Proc. Nat. Sci. Council, R.O.C.*, vol. 19, no. 4, pp. 334–341., July 1995.

[12] G. C. Hwang and S. C. Lin, "A reliable controller for magnetic suspension systems," *Proc. Nat. Sci. Council, R.O.C.*, vol. 19, no. 3, pp. 245–252.

[13] Y. Kanemitsu, M. Ohsawa, and E. Marui, "Comparison of control laws for magnetic levitation," in *Proc. 4th Int. Symp. Magnetic Bearings*, 1994, pp. 13–18.

[14] L. Ljung, *System Identification: Theory for the User*. Englewood Cliffs, NJ: Prentice-Hall, 1987.

[15] Z. Ren and A. Razek, "Modeling of dynamical behaviors of electro-magneto-mechanical coupled systems," in *Proc. 2nd Int. Conf. Computation in Electromagnetics,* Apr. 1994, pp. 20–23.

[16] S. Salcudean and R. L. Hollis, "A magnetically levitated fine motion wrist: Kinematics, dynamics and control," in *Proc. 1988 IEEE Int. Conf. Robotics and Automation*, 1988, pp. 261–266.

[17] J. J. Slotine, "Sliding controller design for nonlinear systems," *Int. J. Control,* vol. 40, no. 2, pp. 421–434, 1984.

[18] J. J. Slotine and W. Li, *Applied Nonlinear Control.* Englewood Cliffs, NJ: Prentice-Hall, 1987.

[19] D. L. Trumper, S. J. Ludwick, and M. L. Holmes, "Design and control of a 6-DOF magnetic/fluidic motion control stage," in *Proc. ASME-IMECE*, San Francisco, CA, 1995, pp. 511–518.

[20] M. Tsuda, Y. Nakamura, and T. Higuchi, "Design and control of magnetic servo levitation," in *Proc. 20th Int. Symp. Industrial Robots*, 1989, pp. 693–700.

[21] M. Tsuda, Y. Nakamura, and T. Higuchi, "Adaptive control for magnetic servo levitation without velocity measurements," in *Proc. 1990 Japan–USA Symp. Flexible Automation*, 1990, pp. 609–616.

[22] ———, "High speed digital controller for magnetic servo levitation of robot mechanisms," in *Proc. 1st Int. Symp. Experimental Robotics*, 1989, pp. 229–243.

[23] V. I. Utkin, "Variable structure systems with sliding modes," *IEEE Trans. Automat. Contr.*, vol. AC-22, pp. 212–222, Mar. 1977.

Hector M. Gutierrez (S'97–M'98) was born in Lima, Peru. He received the B.Sc. degree in applied mathematics in 1989 from the Universidad Cayentano Heredia, Lima, Peru, the B.Sc. degree in mechanical engineering in 1991 from the Ponificia Universidad Catolica, Lima, Peru, and the M.Eng. degree in integrated manufacturing systems engineering in 1993 and the Ph.D. degree in electrical engineering in 1997 from North Carolina State University, Raleigh.

He was a Lecturer in the Department of Mathematics and Physics, Universidad Cayetano Heredia, for two years. He is currently a Postdoctoral Research Associate at the Center for Advanced Computing and Communications, North Carolina State University.

Paul I. Ro was born in Seoul, Korea, in 1959. He received the B.S. degree from the University of Minnesota, Minneapolis, and the M.S. and Ph.D. degrees from Massachusetts Institute of Technology, Cambridge, all in mechanical engineering, in 1982, 1985, and 1989, respectively.

He is currently an Associate Professor in the Mechanical and Aerospace Engineering Department, North Carolina State University, Raleigh. His fields of research are precision machining, magnetic servo levitation, nonholonomic motion planning and control, robotic assembly, and intelligent vehicle control. He is an Associate Editor of *Precision Engineering*.

Dr. Ro is a member of the American Society of Mechanical Engineers and American Society of Precision Engineers.